

Supplementary Information

**Unique emissive behavior of combustion-derived particles under illumination with
femtosecond pulsed near-infrared laser light**

Imran Aslam^a, Maarten BJ Roeffaers^{*a}

^a Centre for Membrane Separations, Adsorption, Catalysis, and Spectroscopy for Sustainable Solutions
Department of Microbial and Molecular Systems
KU Leuven Celestijnenlaan 200F, 3001 Leuven, Belgium

* maarten.roeffaers@kuleuven.be

Materials and methods

Dynamic light scattering (DLS) characterization

Hydrodynamic diameters of the particles suspended in ultrapure water were measured by dynamic light scattering with a ZetaPALS particle analyzer (Brookhaven Instruments Corp., USA). A standard disposable cuvette was used for nanoparticle suspensions to perform the analysis. The measurement data was collected for 2 minutes with multiple measurements on each sample to improve the accuracy.

Scanning electron microscopy (SEM) characterization

To investigate the particle aggregation formation, the nanoparticles were observed using a scanning electron microscope (FEI Quanta 250 FEG) with an acceleration voltage of 20 kV.

Data analysis for emission spectra measurements

For data analysis of emission spectra measurements on CDPs and non-CDPs suspensions, the removal of the background was performed by subtracting the emission spectra of ultrapure water from the emission spectra of CDPs and non-CDPs suspensions.

The data analysis of the emission spectra for dried CDPs and non-CDPs was done as follows: From the lambda stack of all the image frames in each measurement, we obtained the image with maximum pixel intensity. This image was thresholded at 3.5% of the maximum pixel intensity. Afterwards, the pixels below the threshold are set to 0 and above threshold are set to 1 to create a binary image. This binary image was used for pixel-by-pixel multiplication with all the images in the lambda stack. Hence, we obtained a lambda stack after masking, in which the mean intensity of all the pixels above zero is calculated.

The emission spectra are obtained from the mean intensity of all the images in the lambda stack.

Time-correlated single photon counting (TCSPC)

After illumination with fs pulsed laser (810 nm, 80 MHz, 100 fs), the temporal response of the emitted signal from dry CDPs and non-CDPs was recorded using a hybrid detector (HyD-SMD, Leica Microsystems-Germany) after spectral filtering using an Acousto-Optical Beam Splitter (ABOS, Leica Microsystems CMS GmbH – Germany), a dichroic beam splitter (Di02-R442, Semrock Inc., USA), and a bandpass filter (FF01-550/200 nm, Semrock Inc., USA). The hybrid detector was connected to a TCSPC module (HydraHarp 400, PicoQuant GmbH-Germany) which was also synchronized to the pulse train of the laser. The 256x256 pixels images were recorded with a pixel size of 0.72 μm and pixel dwell time of 15.39 μs . All measurements were performed at room temperature. The data were recorded and fitted using SymphoTime64 software (PicoQuant GmbH, Germany). The data were analyzed using Origin (ver. 2020, OriginLab Corporation, USA)

Anti-Stokes and Stokes emission spectra

The Anti-stokes and Stokes emission spectra measurements on CCB were performed on an inverted optical microscope (TiU, Nikon) equipped with a piezoelectric stage on a home-built optical setup. Laser pulses from a femtosecond pulsed laser (MaiTai HP, SpectraPhysics - USA) at 785 nm, 80MHz, 100 fs with an average power of 8 mW were reflected by a dichroic beamsplitter and focused onto the sample with an objective (60x, Plan Flour, N.A. 0.85, Nikon). The anti-Stokes and Stokes emission spectra were collected separately. The laser pulses were reflected by a dichroic beamsplitter (ZT775sp-2p, Chroma - USA) onto the sample, and the anti-Stokes emission spectra from the sample

were collected using the same objective and directed onto a CCD camera (Newton 920, Andor, UK) equipped with a blazed grating monochromator (iHR-320, Horiba, JY) with a grating of 300 g/mm. The signal passed through a 750 nm short pass filter (ET750sp-2p, Chroma - USA). For Stokes emission detection, the laser light is reflected by a dichroic beamsplitter (Di02-R785-25x36, Semrock Inc. USA) and focused onto the sample using the same objective. The signal passed through an 800 nm long pass filter (HQ800LP, Chroma - USA) and was directed to the CCD camera equipped with the grating of 300 g/mm. The slit width was set to 2000 μm . Each spectrum is acquired for 1 second at room temperature.

	Supplier's data Average particle size (nm) [*]	DLS hydrodynamic diameter (nm) Ultrapure water	DLS hydrodynamic diameter (nm) Buffered medium
fCB	<500	363	475
CCB	150	465	420
ufP90	14	201	256
ufPL	13	229	249
CuO	40	2580	567
Fe ₃ O ₄	8	212	1334
Fe ₂ O ₃	6±2	181	1681
TiO ₂	6±2	17	455
SiO ₂	10	23	59

Table S1: Average particles sizes and hydrodynamic diameter of particles in ultrapure water and buffer medium measured using DLS.

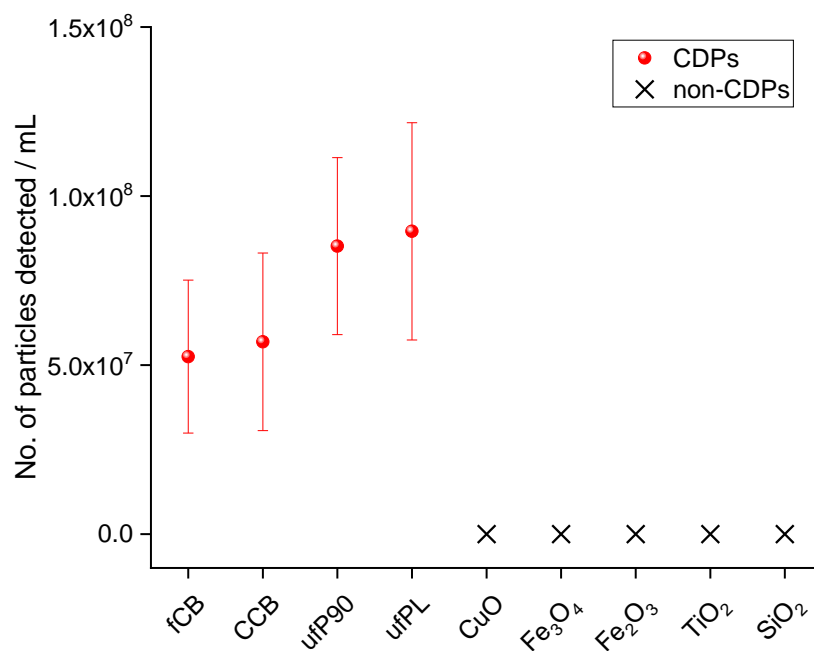


Figure S1: Particles detected per ml in ultrapure water using dual channel detection after illumination with a femtosecond laser at 100 fs, 810 nm and 80 MHz. An average laser power of ~9.5 mW used for the measurements.

The limit of detection (LOD) determined by performing measurements on very low concentrations of CCB in buffer medium based on the calibration curve from Figure S2b¹. The LOD is calculated to be 1.66 $\mu\text{g/mL}$.

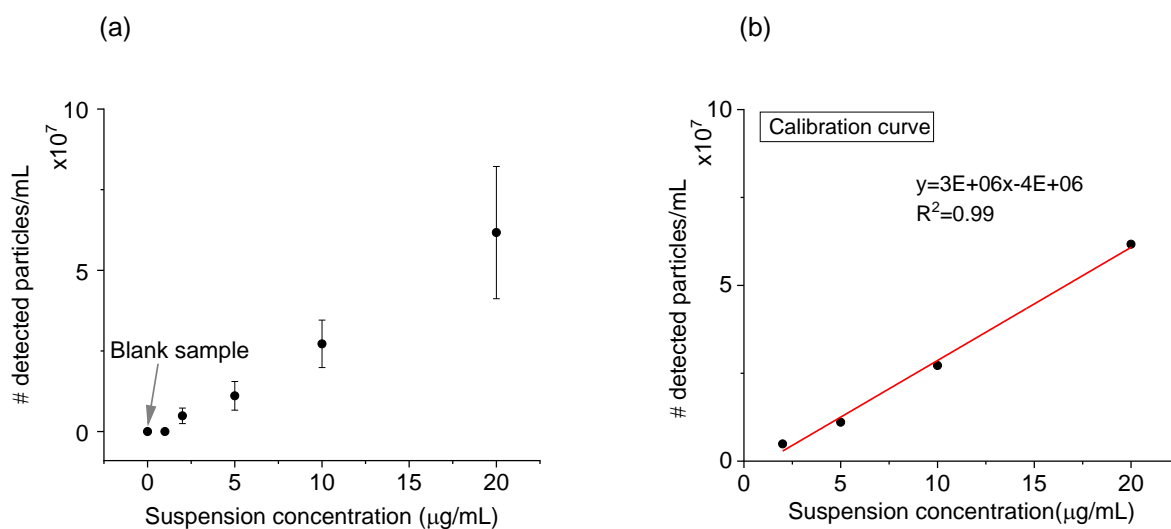


Figure S2: (a) Detected number of particles at different CCB concentrations in buffer medium. Arrow shows that no particles are detected from the blank buffer medium. (b) Linear fit of the calibration curve from 2 $\mu\text{g/mL}$ to 20 $\mu\text{g/mL}$.

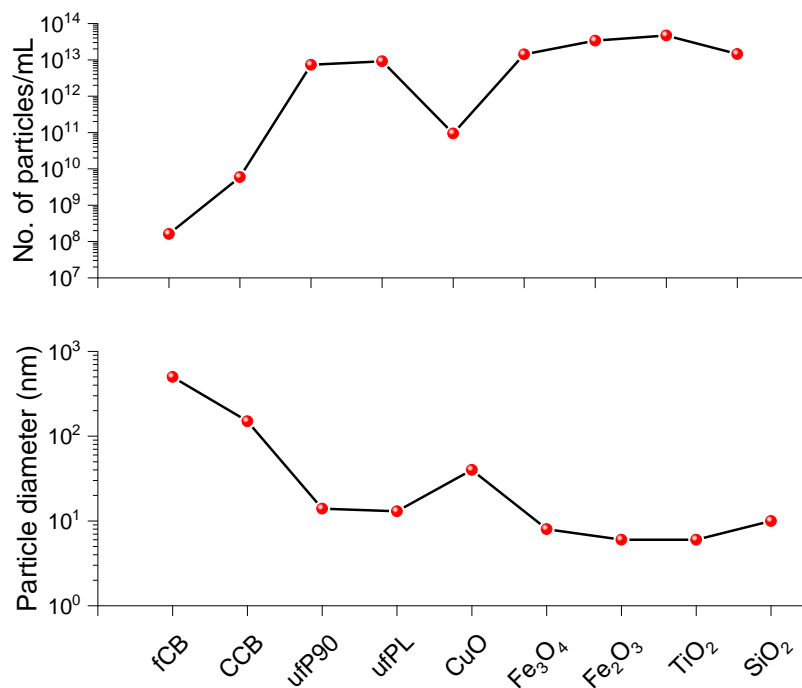


Figure S3: Diameter of the nanoparticles employed in this study based on the manufacturer's data and theoretical calculation of number of particles per ml for concentration of 20 µg/ml. The theoretical calculation for the number of particles per ml is done based on the density of the solution and particle volume.

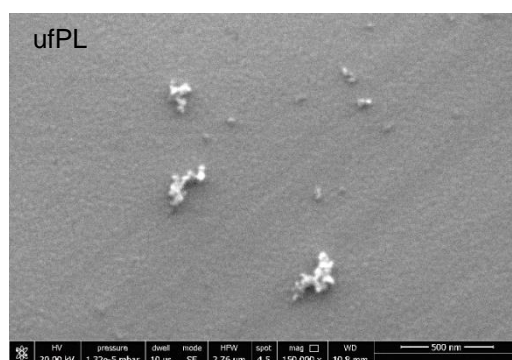
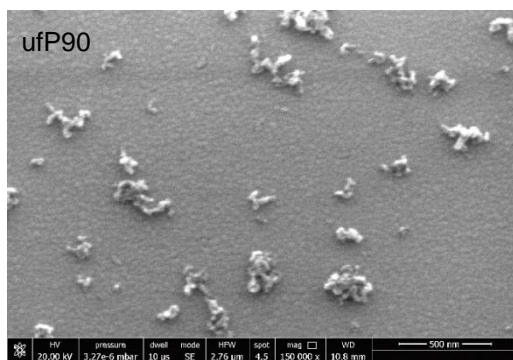
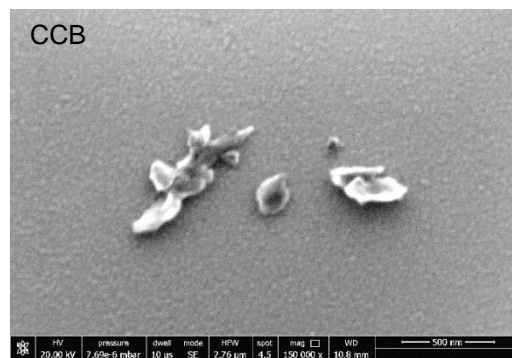
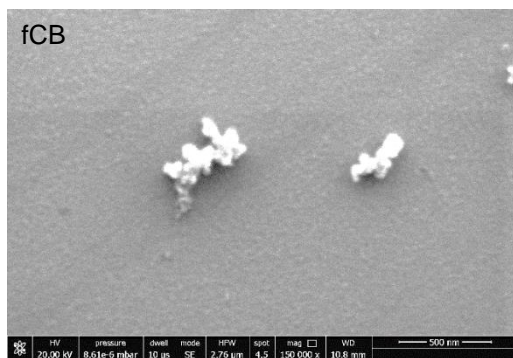


Figure S4: Scanning electron microscopy images of CDPs. These particles tend to form aggregates. Scale bar: 500 nm

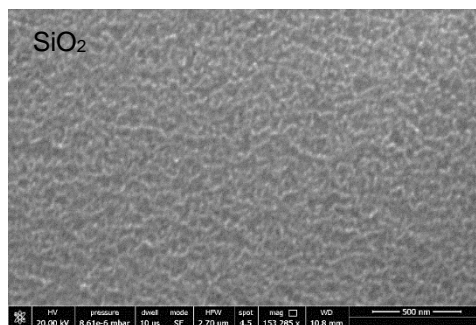
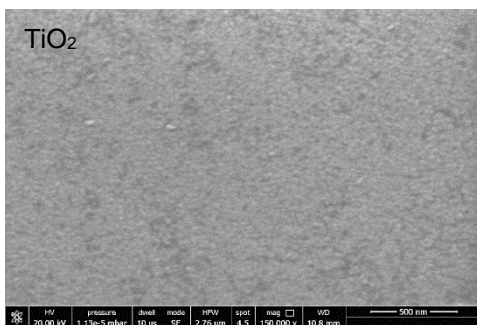
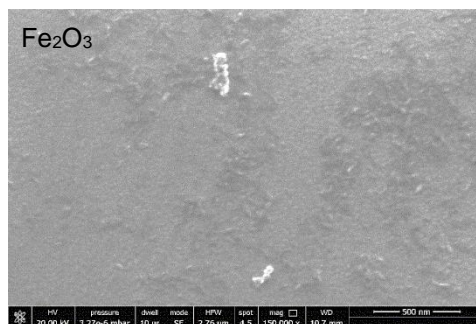
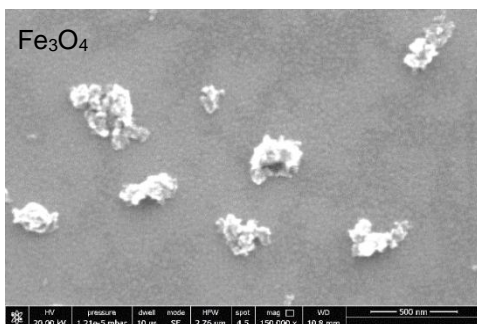
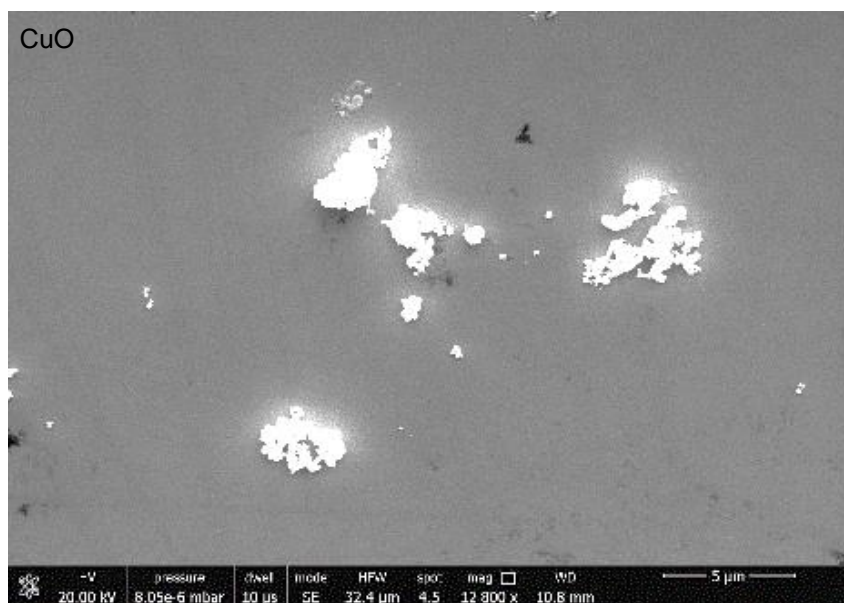


Figure S5: Scanning electron microscopy images of non-CDPs employed in this study showing that non-CDPs also tend to aggregate. Scale bar: 500 nm (CuO: 5 µm).

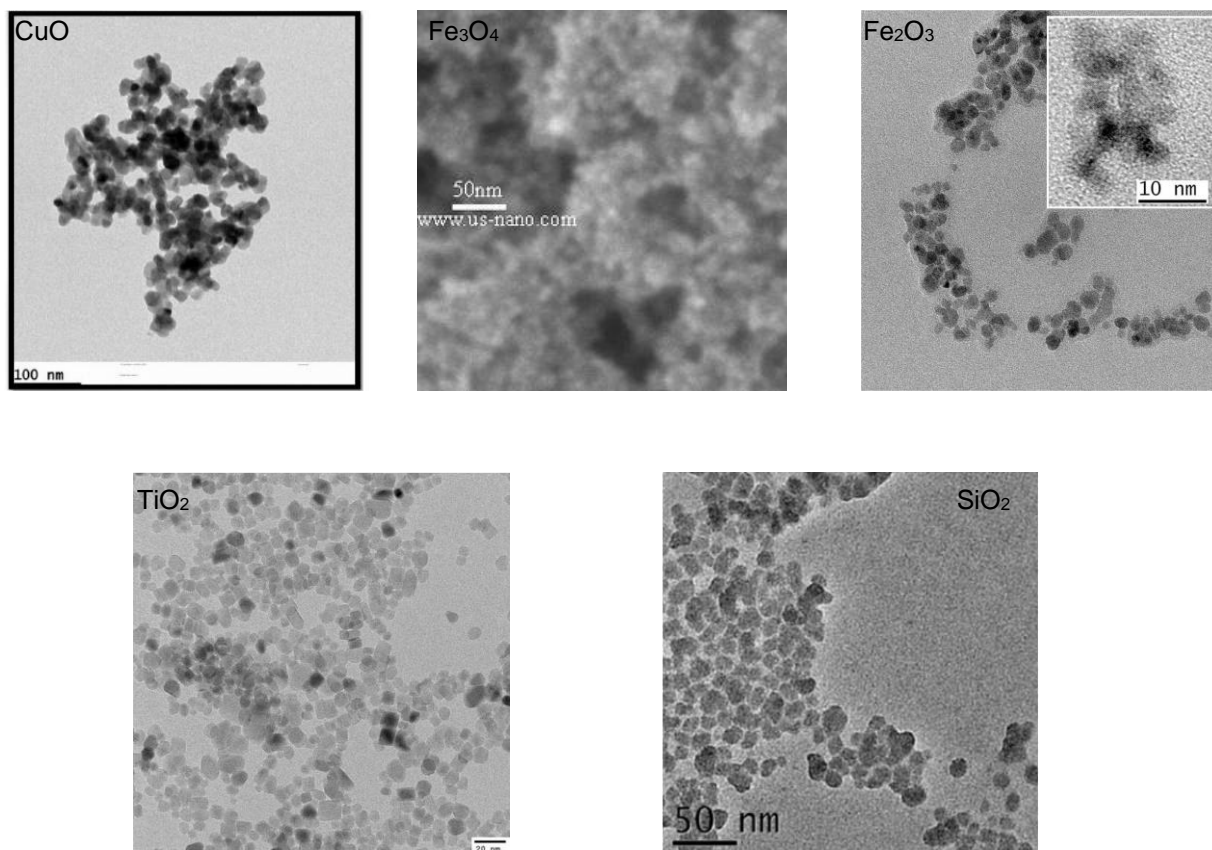


Figure S6: Transmission electron microscopy images of five different types of non-CDPs employed in this study (images from manufacturer).

The TEM images of CDPs can be found from Bové *et al*² article.

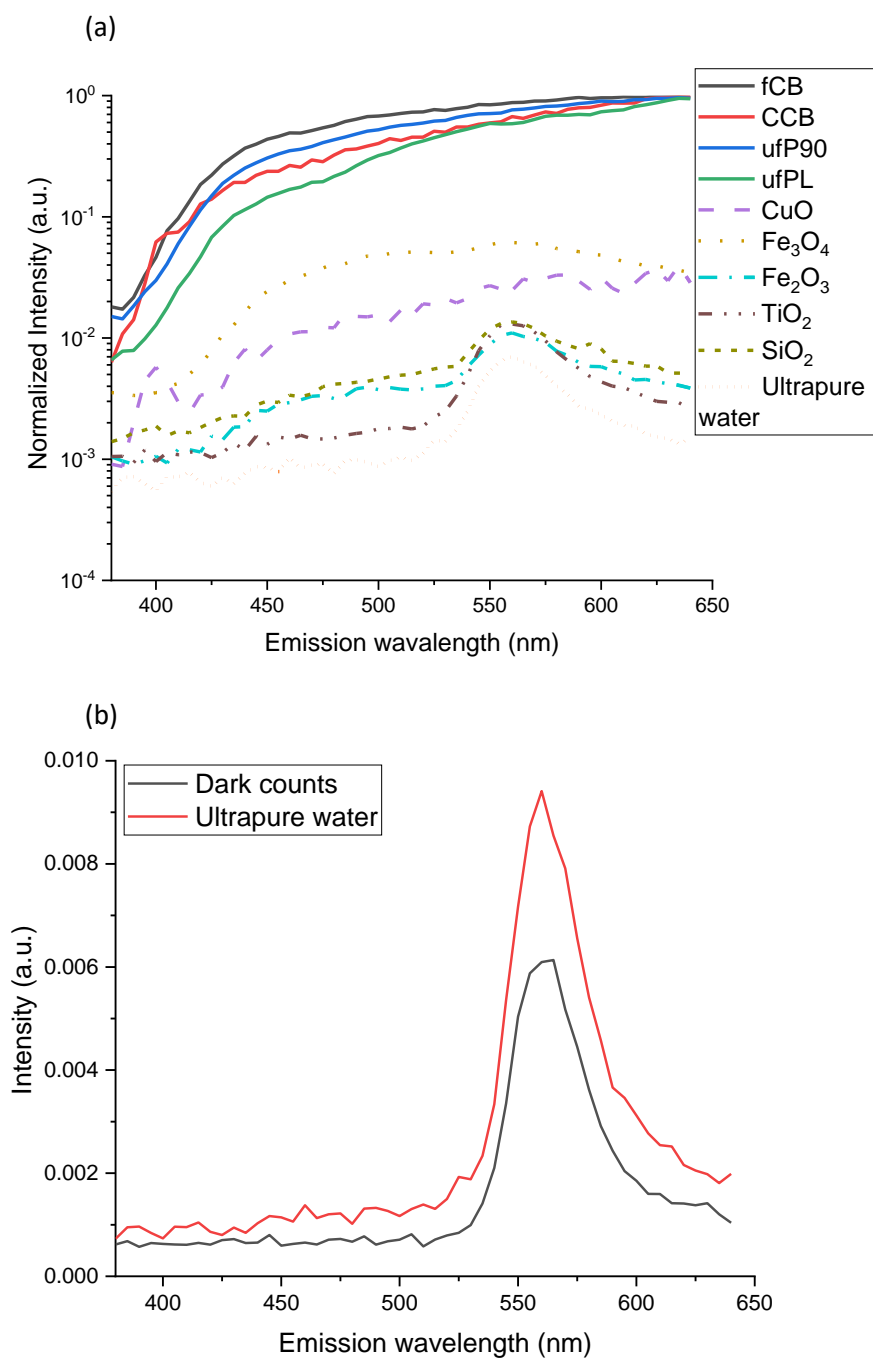


Figure S7:(a) Emission spectra of CDPs and non-CDPs suspensions with background from ultrapure water. (b) Emission spectra recorded for ultrapure water without laser excitation (dark counts) and with laser excitation at 8 mW laser power. The emission spectra without laser excitation show that higher intensity around 550 nm is due to an artifact from the instrument.

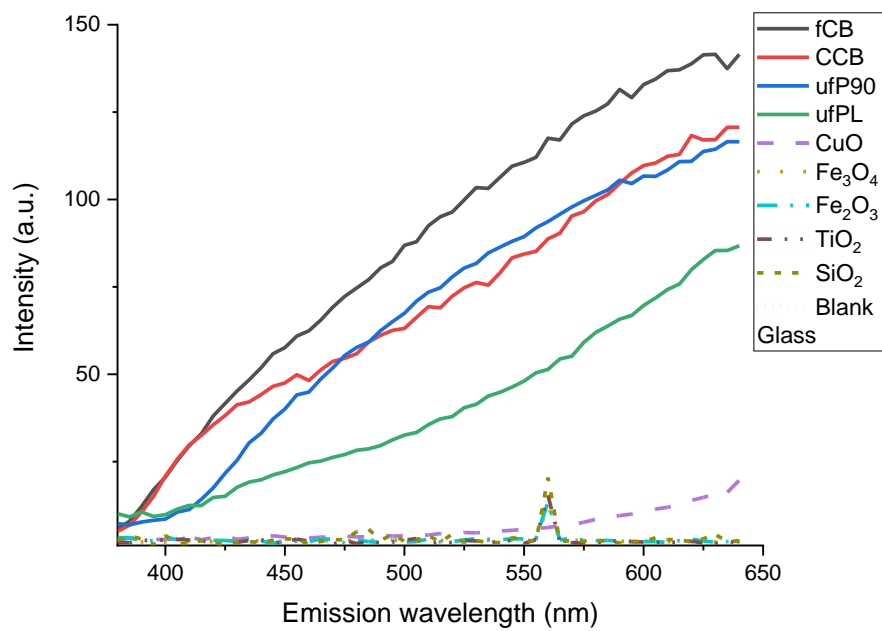


Figure S8: Raw emission spectra of Figure 3d, main article. Emission spectra measurements on dried CDPs and non-CDPs measured using fs-pulsed NIR illumination.

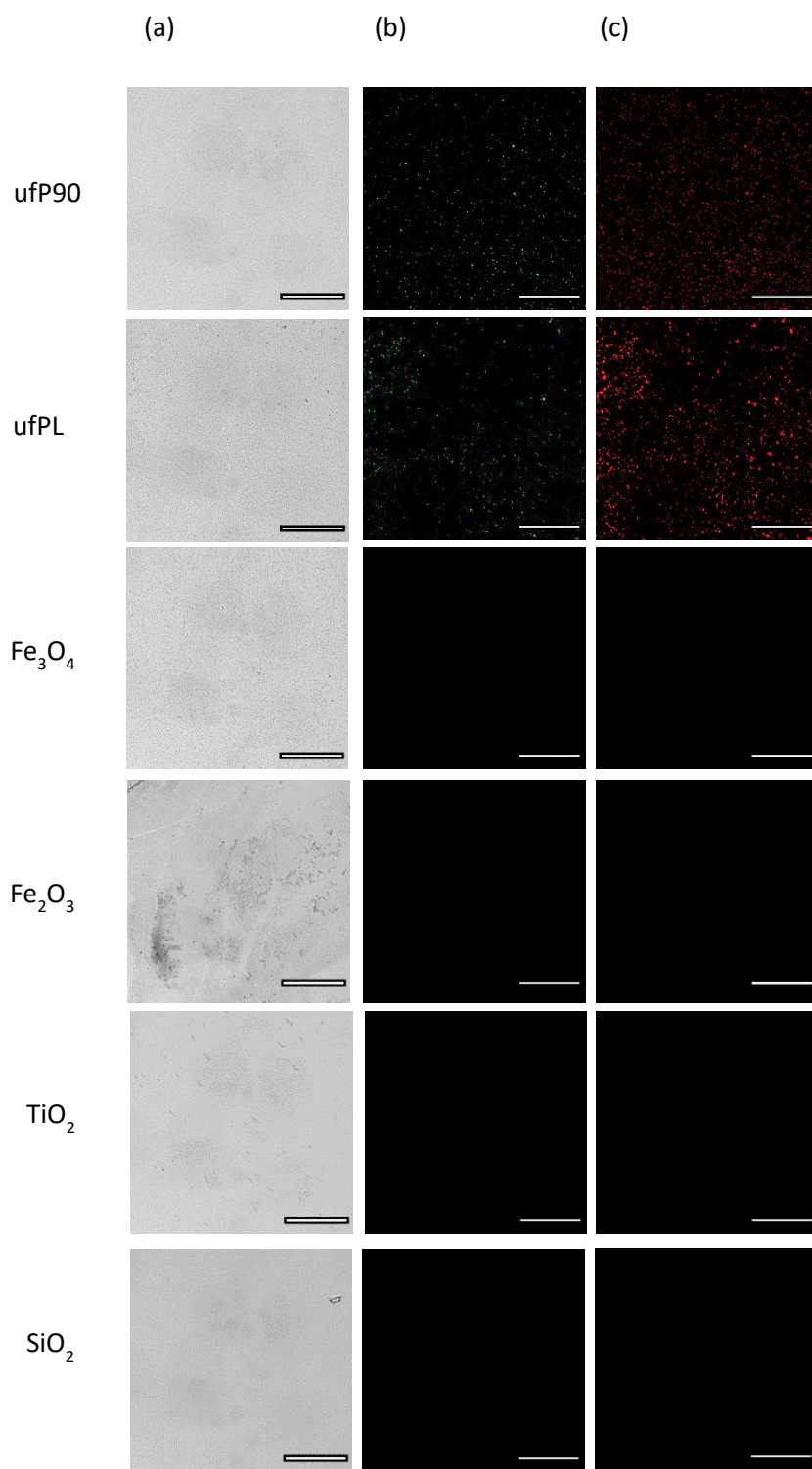


Figure S9: Dual-channel detection of dry CDPs and non-CDPs using fs-pulsed NIR laser illumination at 100 fs, 810 nm and 80 MHz (a) Transmission images of the nanoparticles on a coverglass. (b) Channel 1 images of CDPs and non-CDPs, where CDPs show strong WL emission. (c) Channel 2 images of CDPs and non-CDPs, where CDPs showing very strong emission. The laser power was varied from 1-5 mW to look for an emission signal from non-CDPs. Scale bar: 50 μm

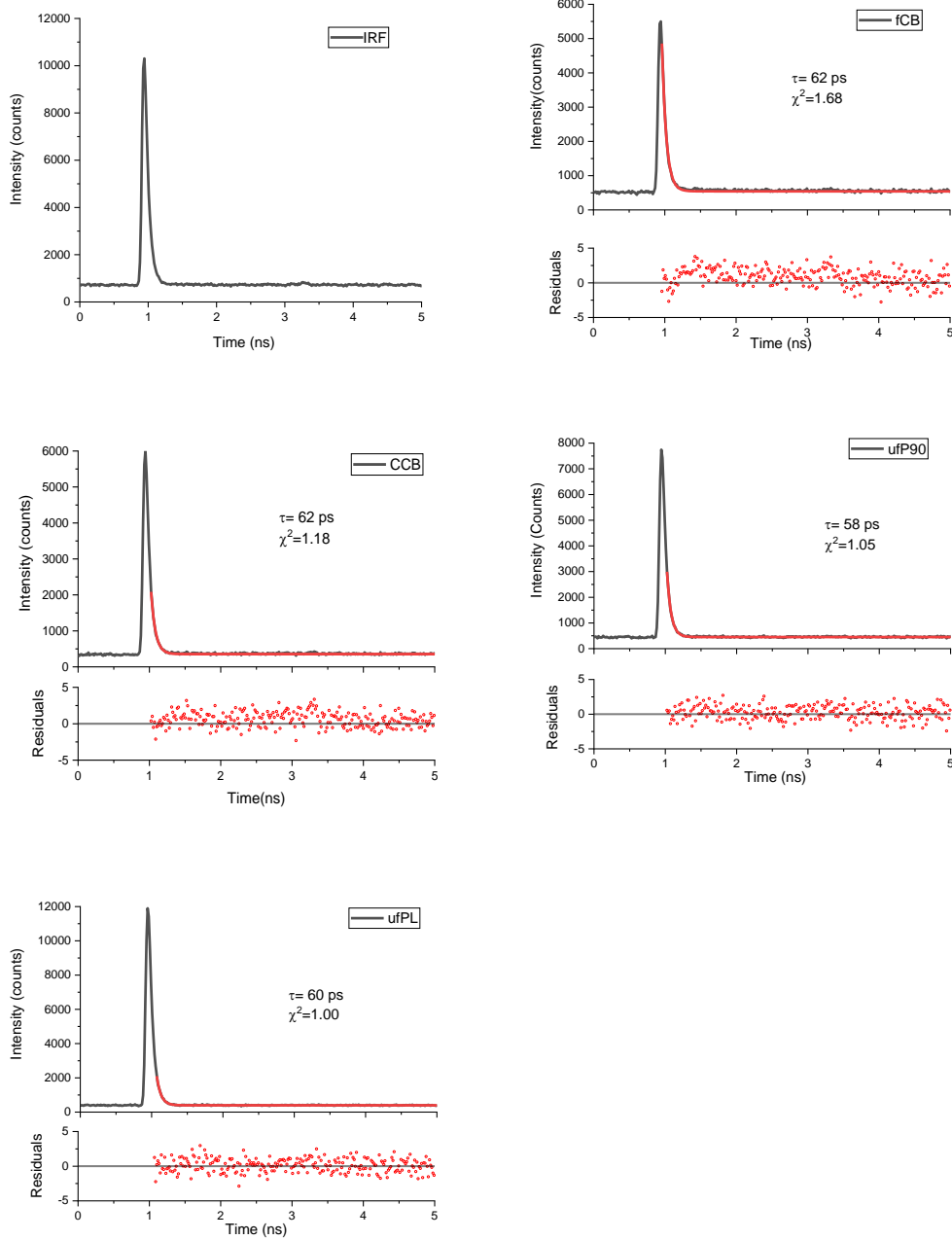


Figure S10: Temporal response of CDPs measured by using time-correlated single photon counting experiments. The instrument response function is shown separately. An average laser power of 1 mW used for CDPs. The data was fitted based on single exponential decay fitting.

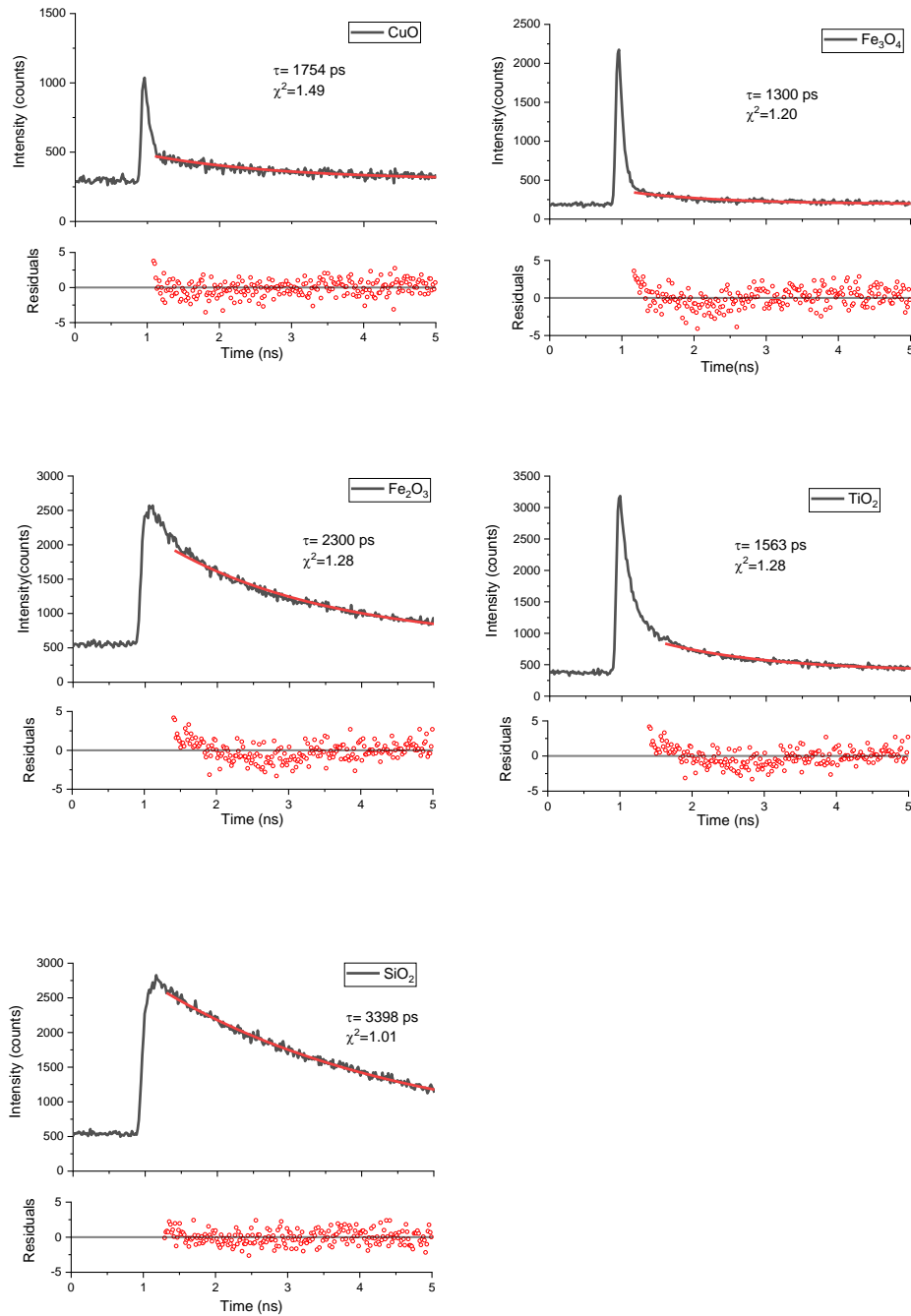


Figure S11: Temporal response of non-CDPs measured by using time-correlated single photon counting experiments. The laser power was varied for non-CDPs to get enough photon counts. The data was fitted based on single exponential decay fitting.

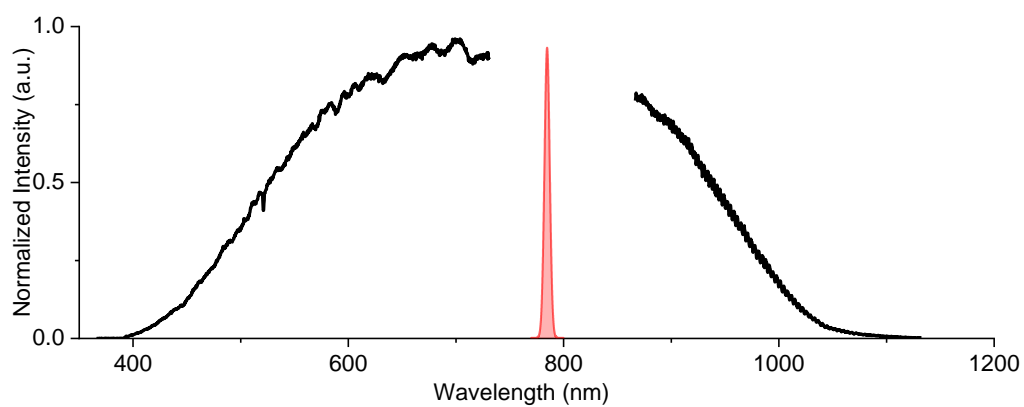


Figure S12: Broad anti-Stokes and Stokes emission spectra of dry CCB nanoparticles under illumination with ultrafast pulses of 100 fs at 785 nm and 80 MHz repetition rate. The laser irradiation (shown in red) is blocked by the filters.

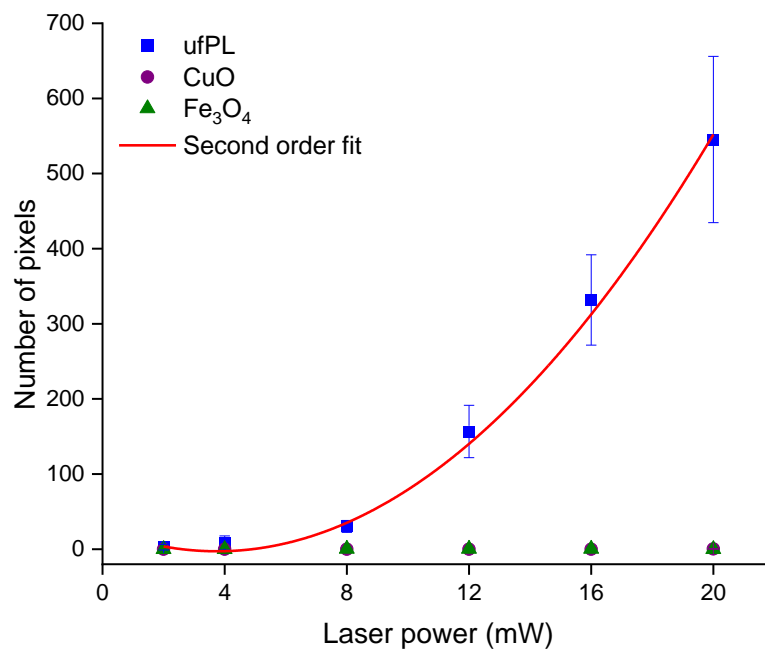


Figure S13: White light emission and laser power dependence for aqueous suspensions (20 $\mu\text{g/mL}$) of ufPL, CuO and Fe_3O_4 . The measurements for the power spectra performed using fs-pulsed NIR laser illumination at 100 fs, 810 nm and 80 MHz. The emission is detected in the spectral range 450-650 nm. To calculate the effective number of pixels in a scan, a constant threshold is set and the number of pixels counted using a MATLAB routine. The data is average \pm standard deviation ($n=3$).

References:

1. Şengül, Ü. Comparing determination methods of detection and quantification limits for aflatoxin analysis in hazelnut. *J. Food Drug Anal.* **24**, 56–62 (2016).
2. Bové, H. *et al.* Biocompatible Label-Free Detection of Carbon Black Particles by Femtosecond Pulsed Laser Microscopy. *Nano Lett.* (2016). doi:10.1021/acs.nanolett.6b00502